

Large Eddy Simulation of Supersonic H₂-O₂ Combustion

Umut Guven and Guillaume Ribert
Normandie Univ., INSA de Rouen, UNIROUEN, CORIA, CNRS
76000 Rouen, France

1 Introduction

Studying the combustion in a liquid rocket engine (LRE) is a challenging task [1]. In particular the ignition process is not well understood. The rocket engine combustion chamber under consideration is composed of a plate of tens of coaxial injectors. In pre-combustion chamber ignition, a small chamber is built next to the main combustion chamber and connected through an orifice [2] as in Vinci engine [3]. This igniter is located in the plate centre and allows repeated starting of engines. A sequence of LRE firing may be summarized as follows: first, the combustion chamber is filled with an inert gas to avoid any hazardous combustion. Then, a high-pressure injection of hydrogen occurs through coaxial injectors for few milli-seconds creating under-expanding jets. Once the chamber is filled with hydrogen, the hot burnt gases coming from the igniter are injected at high-speed. They are produced from the lean combustion of hydrogen with oxygen, i.e. with an excess of oxygen. An additional injection of hydrogen surrounding the igniter is performed to obtain a stoichiometric combustion with the residual oxygen contained in the burnt gases. Finally, the liquid oxygen (LOx) is injected through coaxial injectors and a flame propagates from injector to injector. Hydrogen jet is supersonic during ignition because of the high pressure ratio that results from the low pressure in the main chamber. With the consecutive increase of pressure, such injections will consequently exhibit subsonic velocities. Studying the whole sequence of ignition in a LRE is a scientific challenge that has not been extensively addressed yet. The present study is focused on the simulation of the igniter start and represents the first necessary step towards more complex situations where the initial flame propagates through the combustion chamber and ignites coaxial injectors.

2 Configuration and Mesh Resolution

The modeling of the target configuration is shown in Fig. 1 where the igniter, which is originally surrounded by coaxial injectors, is simulated alone with an hydrogen jet on sides (as in [4]). A focus is then given on the intrinsic igniter characteristics without simulating the prohibitive and complex interaction between igniter and adjacent injectors that would require at least 5 billions of mesh points.

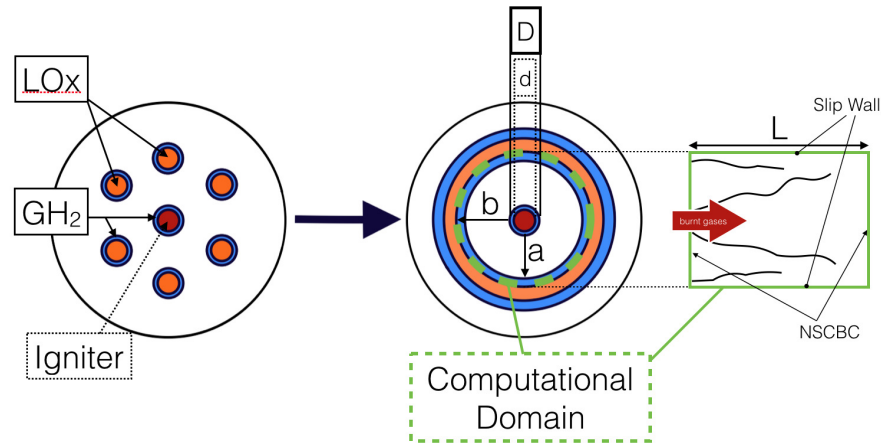


Figure 1: Sketch of the igniter head modeling.

The igniter is a long tube of diameter d that links a small combustion chamber to the main combustion chamber. In the small chamber, the combustion of hydrogen with oxygen in excess occurs at high pressure and the resulting hot burnt gases are delivered at Mach number $M = 1$ into the main chamber [4]. The pressure of injection is close to $p_{inj} = 10$ bar. A hydrogen cooling flow is positioned around the igniter tube (external diameter D). This coolant hydrogen [10] flowing at 200 K is injected in the main chamber at supersonic speed ($M = 1.5$, $p_{inj} = 2$ bar) and reacts with the resulting oxygen coming from the igniter to produce roughly a global stoichiometric combustion. Apart from the igniter are located the first row of coaxial injectors that feature an inner jet of oxygen surrounded by a flow of hydrogen. They are modeled by a single annular ring located at a distance a from the surrounding hydrogen and having length b . The composition of the burnt gases exiting from the igniter results from the combustion of hydrogen with oxygen in excess at 1.0 MPa to yield a temperature between 2000 and 3000 K [11]. An equilibrium calculation performed with the software EQUIL from the CHEMKIN package [12] generated the following composition of species: $Y_{HO_2} = 0.0001$, $Y_{H_2} = 0.0004$, $Y_{O_2} = 0.7577$, $Y_{H_2O} = 0.2299$, $Y_{OH} = 0.0105$ and $Y_O = 0.0014$. The incoming flow is then modeled by 75% of oxygen and 25% of water in mass fraction at a temperature of 2000 K.

Simulations are carried out with the finite volume code SiTCom-B [5] which solves the unsteady compressible reacting Navier-Stokes equation system on Cartesian meshes. SiTCom-B is mainly designed to perform Direct Numerical Simulation (DNS) and highly resolved LES on massively parallel computers. The subgrid scale (SGS) terms are modeled with the dynamic Smagorinsky closure [7] and the modeling of the filtered source term of species is based on the laminar model along with the reduced chemistry of Boivin et al. [9] (5 reacting species and 3 global steps). A mesh cell size (Δx) of $25 \mu\text{m}$ is used everywhere. Constant subgrid Prandtl and Schmidt numbers have been set to unity. Balance equations of species mass fractions, momentum and total non chemical energy are numerically integrated with a 4th-order skew-symmetric-like scheme augmented with a 2nd and 4th-order artificial viscosity for spatial discretization [8]. Time advancement is performed using a 4th-step Runge-Kutta scheme. Finally, inlet and outlet boundary conditions are treated with classical NSCBC [6], which adapt automatically knowing the local Mach number, and side walls are modeled with slip immersed boundary methods. This strategy may be found in [5, 15]. The quality of the

LES simulation was assessed through the Pope criterion (M_E) defined as $M_E = k_{SGS}/[k_{SGS} + k_{RES}]$ where k_{RES} is the resolved turbulent kinetic energy, k_{SGS} is the subgrid scale turbulent kinetic energy and the sum $k_{RES} + k_{SGS}$ is the total turbulent kinetic energy. It was verified that this ratio is below the recommended value of 0.2. Similarly, the impact of the laminar model, i.e. the no-model assumption, was assessed through Da_{sgs} that is defined as the ratio of the characteristic time of the flow (τ_{sgs}) over the characteristic time of chemistry (τ_c). Da_{sgs} was found below unity validating such procedure.

3 Results

Figure 2 shows the temporal evolution ($t = 0.1, 0.2, 0.4, 0.6, 0.8$ and $0.9 \times t_B + 10t_F$ with $t_B = 1.5 \times 10^{-5}$ s and $t_F = 5 \times 10^{-6}$ s) of temperature, heat release rate (HRR), mass fraction of radical H, Mach number and stoichiometric iso-line on a Schlieren field during the ignition process. Stoichiometric iso-line was computed using Bilger's definition of mixture fraction. When the burnt gases start to get into the combustion chamber, the two injectors of hydrogen surrounding the igniter exhibit an under-expanded jet with equivalent barrel shocks and Mach disks. The penetration of the burnt gases strongly affects this structure modifying the angle of jet of hydrogen as in a jet in cross flow. At the early instants of the burnt gases injection (row 1 and 2 of Fig. 2) the flame is not attached to the igniter lips because of the resulting diluent. The burnt gases jet opening occurs with a constant angle until it interacts with the hydrogen jets creating a zone, a supersonic mixing layer (SML), of strong turbulence where the flame takes place. This flame is stuck to the stoichiometric line where the production of radical H and heat release is maximal. A maximum temperature of 3500 K is found that is a common value for stoichiometric hydrogen-oxygen combustion [13]. Hence, the flame exhibits a structure of a diffusion flame from the exit of the igniter duct till the exit of the domain of simulation. This flame also ignites the hydrogen coming from the coaxial injectors as observed, for instance, on flame sides: a pocket of pure hydrogen is wrapped by the flame at $t = 6/10t_B + 10t_F$ and is almost totally consumed at $t = 9/10t_B + 10t_F$. This flame structure is confirmed by the flame index ($F.I.$) of Takeno [14] defined as $F.I. = \vec{\nabla}_{H_2} \cdot \vec{\nabla}_{O_2}$ that is found $F.I. < 0$ everywhere confirming the existence of a diffusion flame (Fig. 3(a)). The position of three discontinuities (D in Fig. 2 on the fourth line for Schlieren field) have been recorded on the igniter jet axis: D₁ is the primary shock generated by the injection of burnt gases; D₂ is the stoichiometric iso-line; D₃ is the discontinuity associated to the under-expanded jet of the igniter. In Fig. 3(b), D₁ exhibits a constant velocity of $c_{LES} = 1890$ m/s. Theoretically, this configuration is equivalent to the solution of the problem of Sod: the shock velocity is given by $c_{th} = V_{inj}\rho_1/(\rho_1 - \rho_2)$ where V_{inj} is the jet velocity (1000 m/s), ρ_1 is the density behind the discontinuity and ρ_2 , the density in front of the discontinuity. The analytical solution gives $c_{th} = 1830$ m/s that represents a difference of 3% with c_{LES} . This observation means that the level of turbulence generated by the jet of hydrogen has no impact on the primary shock evolution.

This is confirmed when performing a non-reacting case, i.e. when chemical reactions are deactivated: D₁ exhibits the same constant velocity than for the reacting case. Moreover, D₂ and D₃ have the same behavior for $t^+ \leq 0.35$. Then, these two discontinuities split because of the transverse shocks generated by the instability (vortex ring) initially created when the burnt gases start to be injected. A difference between the reacting and non-reacting cases occurs at $t^+ = 0.6$ because the shocks arrangement must adapt to a SML with augmented instabilities and turbulence. The presence of the turbulent diffusion flame in the SML modifies the structure of the incoming supersonic jet of burnt gases. An oblique shockwave is then created in front of the flame, i.e. with a SML having a higher temperature and viscosity, and its position differs from the oblique shockwave observed in front of the SML in the non-reacting case. In Fig. 2 this discontinuity

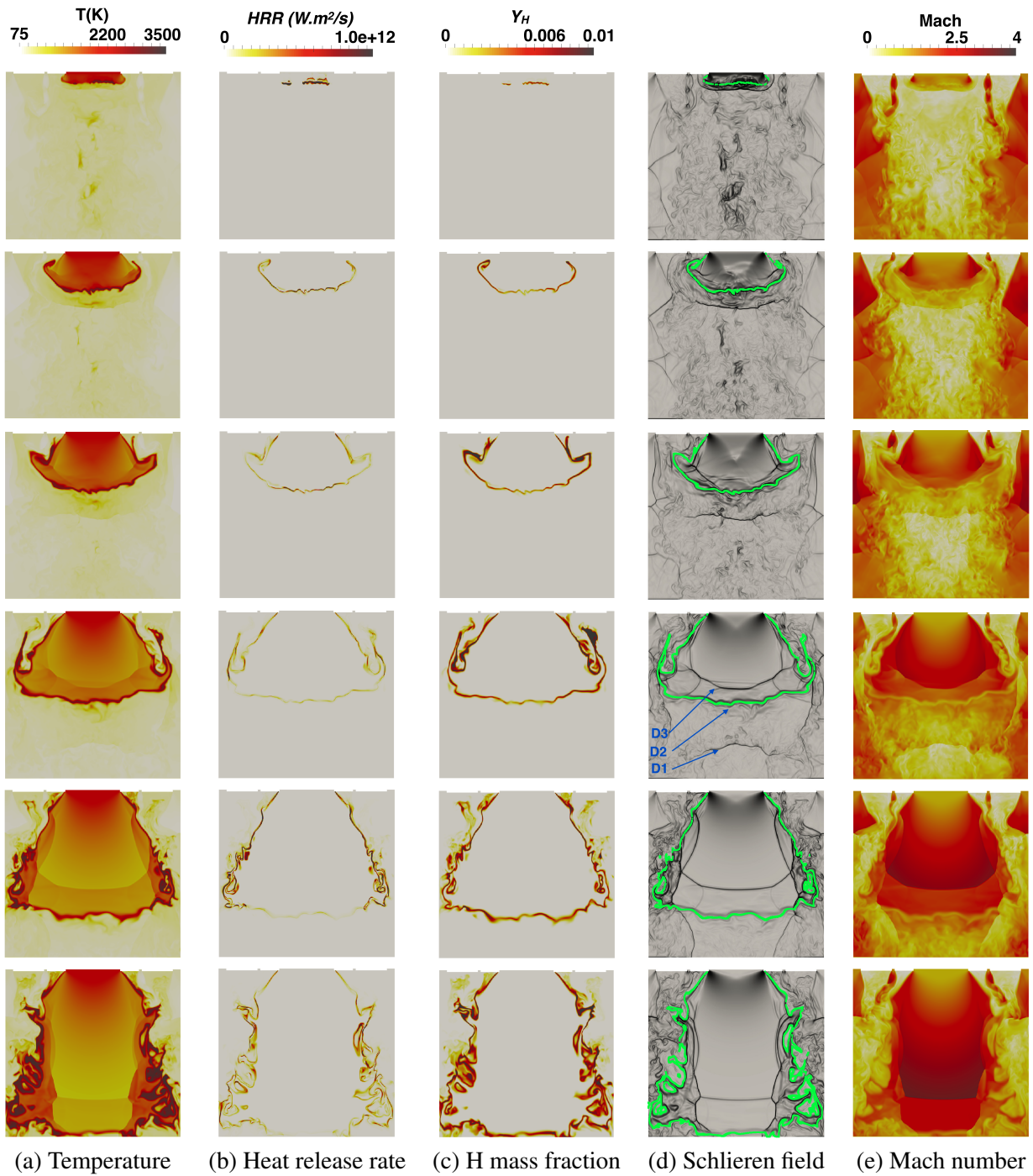


Figure 2: 2D slices of the instantaneous 3D field during burnt gases jet. From top to bottom, $t = 0.1, 0.2, 0.4, 0.6, 0.8$ and $0.9 \times t_B + 10t_F$ with $t_B = 1.5 \times 10^{-5}$ s

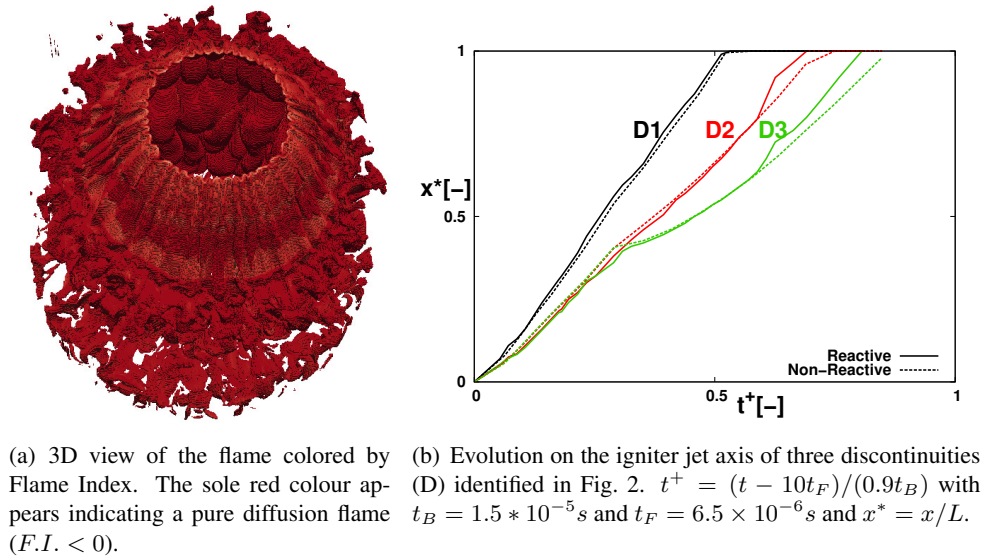


Figure 3: Igniter characteristics.

adapts continuously to the turbulent flame movement. The driving physical phenomenon of this ignition configuration is then an aerodynamic effect. In addition, the combustion is sustained by the surrounding injector of hydrogen and yields enough energy to create reacting zones with hydrogen coming from coaxial injectors.

4 Conclusion

Studying the ignition process of a rocket engine is fundamental for the understanding of the firing of coaxial injectors. The large-eddy simulation of supersonic H_2/O_2 combustion is performed for a simplified configuration of rocket-like igniter. The study is a supersonic injection of burnt gases (hot oxygen and water) in a combustion chamber filled with hydrogen. Simulations are performed with the multi-species reactive solver SiTCom-B. The different ingredients required to perform with success such challenging simulation has been addressed. The 3D large-eddy simulation is performed for a mesh resolution of $25 \mu m$. Pope's criterion (M_E) is respected ($M_E < 0.2$). The first stage of the ignition sequence has been simulated introducing hydrogen into a quiescent chamber full of an inert species such as helium or nitrogen. A complex flow organization is found with multiple interactions between shocks and turbulence. The structure of an under-expanded jet that resembles to a barrel-shock shape is found for the hydrogen jet surrounding igniter. The second stage of the ignition sequence, i.e. the introduction of lean hot burnt gases, has been simulated with the use of a laminar combustion model, i.e. $\tilde{\omega}_k(\cdot) = \dot{\omega}_k(\tilde{\cdot})$ that respected the criterion $Da_{sgs} < 1$. The injection of burnt gases into the chamber shows a diffusion flame structure attached to the igniter soon after the injection of burnt gases and interacting with the different streams of hydrogen. The flame is located in the supersonic mixing layer and little affects the burnt gases expansion meaning that the aerodynamic effect of the injection of burnt gases plays a major role in flame establishment.

5 Acknowledgments

Umut Guven was funded by Région Normandie. Dr. Guillaume Ribert was supported by the project RE-FINE (ANR-13-BS09-0007).

References

- [1] Yang V, Habiballah M, Hulka J, Popp M. (2004). *Liquid Rocket Thrust Chambers: Aspects of Modeling, Analysis, and Design*, AIAA Edt.
- [2] Sutton G, Biblarz O. (2010). *Rocket Propulsion Elements*, 8th ed., Wiley-Interscience.
- [3] Frenken G, Vermeulen E, Bouquet F, Sanders B. (2002). Development Status of the Ignition System for Vinci. AIAA P. 2002-4330.
- [4] Hensel C, Wiedmann D, Oechslein W, Gorgen J. (2002). Ignition Aspects for the Vinci Thrust Chamber. AIAA P. 2002-4008.
- [5] Petit X, Ribert G, Lartigue G, Domingo P. (2013). Large-Eddy Simulation of Supercritical Fluid Injection. *J. Supercritical Fluids*. 84: 61–73.
- [6] Poinso T, Veynante D. (2012). *Theoretical and Numerical Combustion*, 3rd ed.
- [7] Lilly D. (1991). A Proposed Modification of the Germano Sub-grid Scale Closure Method. *Phys. Fluid.* 4(3): 633–635.
- [8] Ducros F, Laporte F, Souleres T, Guinot V, Moinat P, Caruelle B. (2000). High-Order Fluxes for Conservative Skew-Symmetric-like Schemes in Structured Meshes: Application to Compressible Flows. *J. Comput. Phys.* 161(1): 114–139.
- [9] Boivin P, Jimenez C, Sanchez A, Williams F. (2011). An Explicit Reduced Mechanism for H₂-air Combustion. *Proc. Combust. Inst.* 33(1): 517–523.
- [10] Ribert G, Taieb D, Yang V. (2015). Large-Eddy Simulation of a Supercritical Channel Flow using a Shock Capturing Numerical Scheme. *Comput. Fluids*. 117: 103–113.
- [11] Lacaze G. (2009). *Simulation aux Grandes Echelles de l’Allumage de Moteurs Fuses Cryotechniques*. Ph.D. thesis. Univ. Toulouse, France.
- [12] Kee R, Rumpley F, Miller J (1989). *Chemkin-II: A Fortran Chemical Kinetics Package for the Analysis of Gas Phase Chemical Kinetics*. SAND89-9009B.
- [13] Ribert G, Zong N, Yang V, Pons L, Darabiha N, Candel S. (2008). Counterflow Diffusion Flames of General Fluids: Oxygen/Hydrogen Mixtures. *Combust. Flame*. 154(3): 319–330.
- [14] Yamashita H, Shimada M, Takeno T. (1996). A Numerical Study on Flame Stability at the Transition Point of Jet Diffusion Flames. *Symp. Int. Combust.* 26(1): 27–34.
- [15] Petit X, Ribert G, Domingo P. (2015). Framework for Real-Gas Compressible Reacting Flows with Tabulated Thermochemistry. *J. Supercritical Fluids*. 101: 1–16.